Relaxing the Initial Model Constraint for Crustal-Scale Full-Waveform Inversion with Graph Space Optimal Transport Misfit Function

A. Górszczyk[1,2], L. Métivier[1,3], R. Brossier[1]

[1] Univ. Grenoble Alpes, ISTerre; [2] Institute of Geophysics, PAS; [3] CNRS, Univ. Grenoble Alpes, LJK

Summary

We investigate the potential of the recently proposed Graph-Space Optimal Transport (GSOT) misfit function, to mitigate the cycle-skipping problem at the initial stage of the crustal-scale Full-Waveform Inversion (FWI) from the wide-angle stationary-receiver seismic data. Ultra-long offset seismic data contain very rich information about the deep crust, recorded along the various diving, refracted and reflected wavepaths. This diversity of the arrivals representing different propagation regimes - combined with relatively sparse receiver spacing - increases the non-linearity of the inverse problem and makes it difficult to find the initial FWI model which satisfies the cycle-skipping criterion. Here we search for the panacea to this problem through the application of more convex misfit function - namely GSOT. We apply the acoustic time-domain FWI to the synthetic marine seismic dataset generated in the realistic model of the complex subduction zone. We show that FWI with GSOT misfit function, combined with proper data selection, allows for reconstruction of the true velocity model starting from the simple 1D initial model. Despite the significant cycle-skipping problem at the initial stage of inversion, the GSOT misfit function is still able to overcome local minima and guide the inversion toward the correct solution.

Introduction

Long-offset stationary-receiver seismic data are routinely employed for the imaging of the deep geological targets. The ability to register low-frequency, multi-component data makes this kind of acquisition suitable for the inverse methods such as Full Waveform Inversion (FWI). This is because the information collected along the diving and refracted wavepaths, additionally enriched with the wide-angle reflections, has a great potential to efficiently constrain the subsurface velocity at depths which are beyond the range of the typical reflection streamer data.
However, the rich information carried by different arrivals naturally increases the non-linearity of the inverse problem. This in turn rises the possibility of cycle-skipping and can guide FWI towards local minima. The problem is especially severe at the initial stage of FWI, when the accuracy of the starting model plays a key role for the successful inversion process. To overcome this issue during FWI of long-offset data, one can consider different approaches including: (i) building more accurate initial models e.g. with slope tomography (Sambolian et al., 2018); (ii) expanding the search space by relaxation of the wave-equation constraint (Aghamiry et al., 2018); or (iii) mitigating the FWI non-linearity using Laplace-Fourier FWI (Górszczyk et al., 2017). On the other hand, the cycle-skipping problem can be mitigated through the development of global optimization inversion schemes and more convex cost-functions. In particular, recently proposed Graph-Space Optimal Transport (GSOT) misfit function has demonstrated promising results in terms of velocity model reconstruction (Métivier et al., 2019). Comparing to the classical L^2 norm, GSOT is convex with respect to the patterns in the waveform which can be shifted in time for more than half-period. Therefore with proper data-selection strategy, this misfit-function has potential to reduce the risk of cycle-skipping.
To further investigate the GSOT technique, here we apply the time-domain acoustic FWI with GSOT misfit functions to the 2D sparse wide-angle stationary-receiver marine seismic dataset. We assess the potential of GSOT to overcome the cycle-skipping problem at the initial stage of the inversion. As a benchmark we use GO_3D_OBS synthetic model (Górszczyk and Operto, 2020) representing complex geological setting of the subduction zone. Using GSOT combined with the multiscale FWI strategy, we reconstruct in details the underlying structure starting from a simple 1D velocity model. We show that despite the obvious cycle-skipping problem in the initial FWI model, the GSOT misfit function is still able to match corresponding data-samples and converge towards correct solution.

GSOT misfit function

In this study we follow the GSOT strategy presented in Métivier et al. (2019). First we define a seismic trace $d(t)$ discretized as $(d_1,...,d_n)$. We denote its discrete graph by $(t,d) = ((t_1,d_1),\ldots,(t_N,d_N)) \in \mathscr{R}^{2N}$. Let now d_{cal} and d_{obs} be a calculated and observed trace respectively. With (t,d_{cal}) and (t,d_{obs}) we denote their discrete graphs consisting of N delta Dirac functions in the 2D space. The GSOT distance between d_{cal} and d_{obs} is given by solving the linear sum assignment problem:

$$h_2(d_{cal},d_{obs}) = \min_{\sigma\in S(N)} \sum_{i=1}^{N} c_{i,\sigma(i)}(d_{cal},d_{obs}), \tag{1}$$

where $S(N)$ denotes the space of permutation of $\{1,\ldots,N\}$, and c_{ij} is the distance between the points i and j of the discrete graph of d_{cal} and d_{obs}:

$$c_{ij}(d_{cal},d_{obs}) = |t_i - t_j|^2 + |\frac{\tau}{A}\left(d_{cal,i} - d_{obs,j}\right)|^2. \tag{2}$$

In Equation 2, A is the maximum peak amplitude difference between observed and calculated data, while τ is the maximum estimated time shift between d_{obs} and d_{cal}. This ensures the convexity of the GSOT distance for time up to around τ. The assignment problem is efficiently solved using the auction algorithm (Bertsekas and Castanon, 1989). The final cost-function we use for the purpose of FWI application with N_s shots containing N_r receivers is defined as:

$$\min_m f[m] = \sum_{s=1}^{N_s}\sum_{r=1}^{N_r} w^{s,r} h_2\left(d_{cal}^{s,r}[m], d_{obs}^{s,r}\right), \tag{3}$$

where $d_{obs}^{s,r}$ and $d_{cal}^{s,r}[m]$ are the observed and synthetic (calculated in model m) traces respectively associated with source s and receiver r. The $w^{s,r}$ is a trace-by-trace weighting factor, typically used to restore the AVO trend in the data which is removed prior to the calculation of the GSOT cost-function.

FWI setup

In this study we use the 2D V_p and ρ models from the GO_3D_OBS crustal-scale model of the subduction zone (see Figure 1a). The model was designed to benchmark different tomographic and inversion approaches from the field of the seismic imaging with the special emphasize on the FWI of the long-offset stationary-receiver data. Our acquisition setting comprises 72 receivers distributed along the seabed with 2 km spacing intervals as presented in Figure 1a and 1500 shots distributed at each 100 m (from 5 km to 155 km). We use time-domain acoustic modelling with 2 Hz Ricker source-wavelet to generate the synthetic dataset (20 s propagation time). The complexity of the structure is clearly reflected by the various interfering arrivals in the gather presented in Figure 1c.

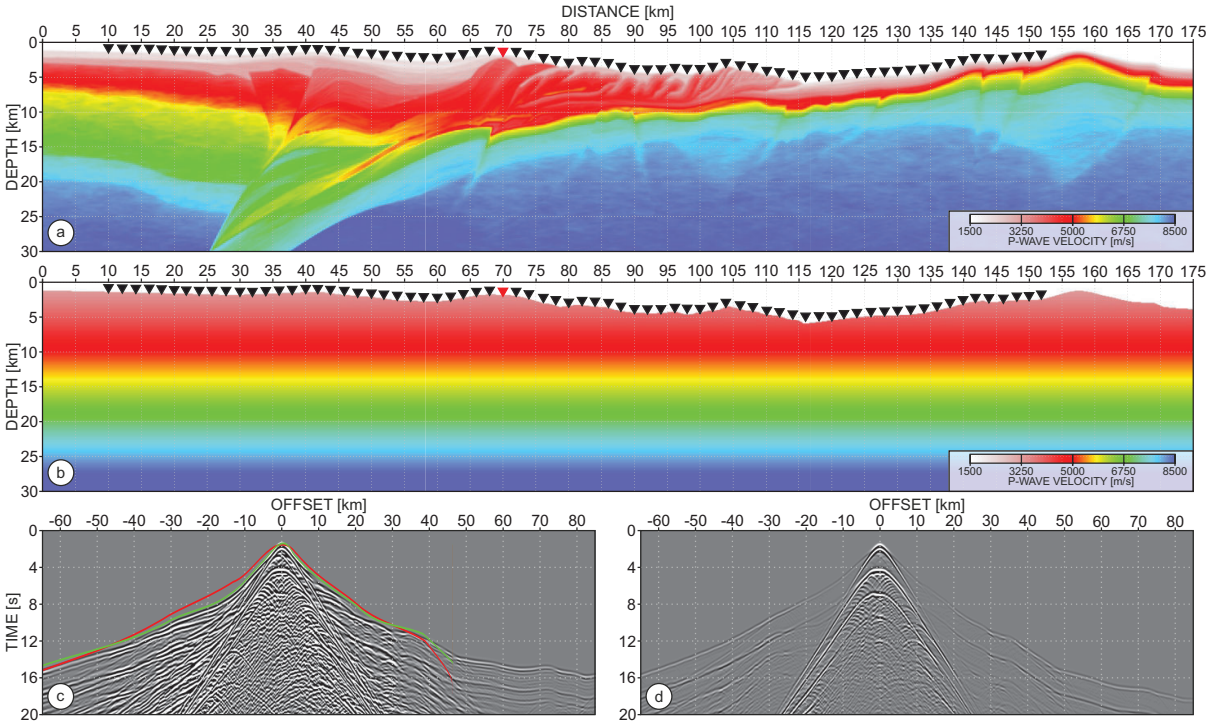

Figure 1 *(a) True and (b) initial V_p models. (c)-(d) Common receiver gathers recorded at 70 km of model distance in (a) and (b) respectively. Green/red lines mark the first breaks in true/initial data.*

As an initial V_p model for FWI we use the simple 1D linear gradient as presented in Figure 1b while we keep the true ρ model during the inversion. The corresponding initial data are presented in the Figure 1d. We perform time-domain acoustic FWI with LBFGS optimization scheme and approximate Hessian matrix for gradient scaling. We invert for the synthetic data without applying any band-pass filter, and we follow the 4-STAGE multiscale strategy (see Table 1) based on the progressively extended time-windows and reduced gradient smoothing. At the initial stage we use trace normalized seismograms, to boost the contribution of the far-offset data penetrating in the deeper parts of the model.

	STAGE1	STAGE2	STAGE3	STAGE4
Time window	0.2 s + 0.5 s taper	0.2 s + 0.5 s taper	0.2 s + 10 s taper	Full data
Amplitude	Trace-normalized	True	True	True
Smoothing	2.0×2.0	1.6×0.8	0.8×0.4	0.8×0.4
Iterations	50	20	150	150

Table 1 *Summary of the inversion steps in the synthetic test*

To analyse the convexity of the GSOT at the STAGE 1 of our inversion, we generate the population of 10 V_p models V_α according to the formula $V_\alpha = (1-\alpha)V_{true} + \alpha V_{init}$ where $\alpha = [0.0, 0.1, 0.2, \ldots, 1.0]$. For each model we calculate the initial misfit function value using $\tau = 0.005$ s and $\tau = 4$ s. The first value of τ mimics the L^2 norm, since the data-sampling in our test equals 0.005 s. The second value of τ was empirically picked to account for significant time-shifts between the early arrivals in true and initial data. The normalized values of the misfit functions are plotted in Figure 2. One can observe that for $\tau = 0.005$ s the local minimum valley starts at $\alpha \sim 0.3$, while for $\tau = 4$ s the inversion is still within global minimum - even when $\alpha = 1.0$ (1D model).

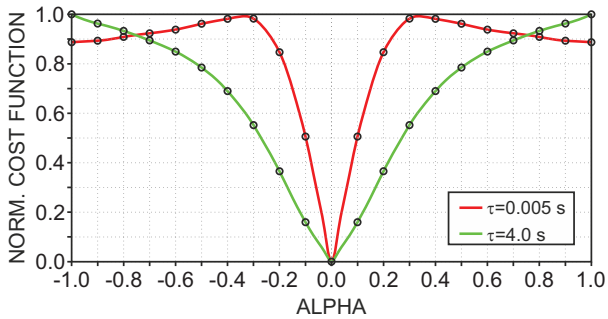

Figure 2 *GSOT cost-function convexity for $\tau = 0.005$ s and $\tau = 4$ s at the STAGE 1 of our test.*

Results

The final recovered V_p model is presented in Figue 3a. Despite relatively sparse receiver spacing and low frequency content, one can observe that the complex velocity structure presented in Figure 1a was recovered in details. In particular, on the landward part the steeply dipping faults marking old backstop around 30-40 km distance as well as thin subduction channel on top of the oceanic crust between 40 and 55 km distance are clearly imaged. In the central part, the accretionary wedge containing sequence of various thrusts is clearly reconstructed including also the low-velocity zone at 12 km depth between 60 and 80 km distance. In the trench part the rapid increase of velocity is properly recovered and sharp contrast of velocity between sediments deposited in the trench and the top of the oceanic crust is imaged. Furthermore, the signatures of the faults cutting through the subducting crust and the upper mantle are also imaged. In the deeper parts of the mantle we start observing some velocity mismatches which possibly results from the limited and mainly sub-horizontal illumination of those segments. This is confirmed by the Figure 3b where we show the logs (marked in Figure 3a with black-dashed lines) representing true (red line) and reconstructed (green line) V_p perturbations (difference between true/initial and reconstructed/initial V_p models). One can observe that the logs remain in very good agreement even for the most complex structures down to around 20 km of model depth, while for the deeper parts some deviations can be observed.
In Figure 3c and d we show initial and final data-fitting comparison. Red-blue color-scale corresponds to the calculated data, while black-coloured phases denote observed data. The scale of the cycle-skipping in Figure 3c is clearly significant. In spite of it, the fact that there is no red color in Figure 3d indicates that presented approach based on the GSOT misfit function led to precise data and model reconstruction.

Conclusion

The GSOT misfit function proves the ability to mitigate the inaccuracy of the initial FWI model. While fulfilling the cycle-skipping condition for long-offset data is challenging, the GSOT technique combined with proper selection of early arrivals allows to maintain the convexity of the cost-function even when the initial data are shifted for more than few cycles with respect to the observed data. We believe that further developments of the OT-based misfit functions can significantly reduce the constraints on the starting model accuracy and reduce the overall risk of cycle-skipping during FWI of wide-angle data.

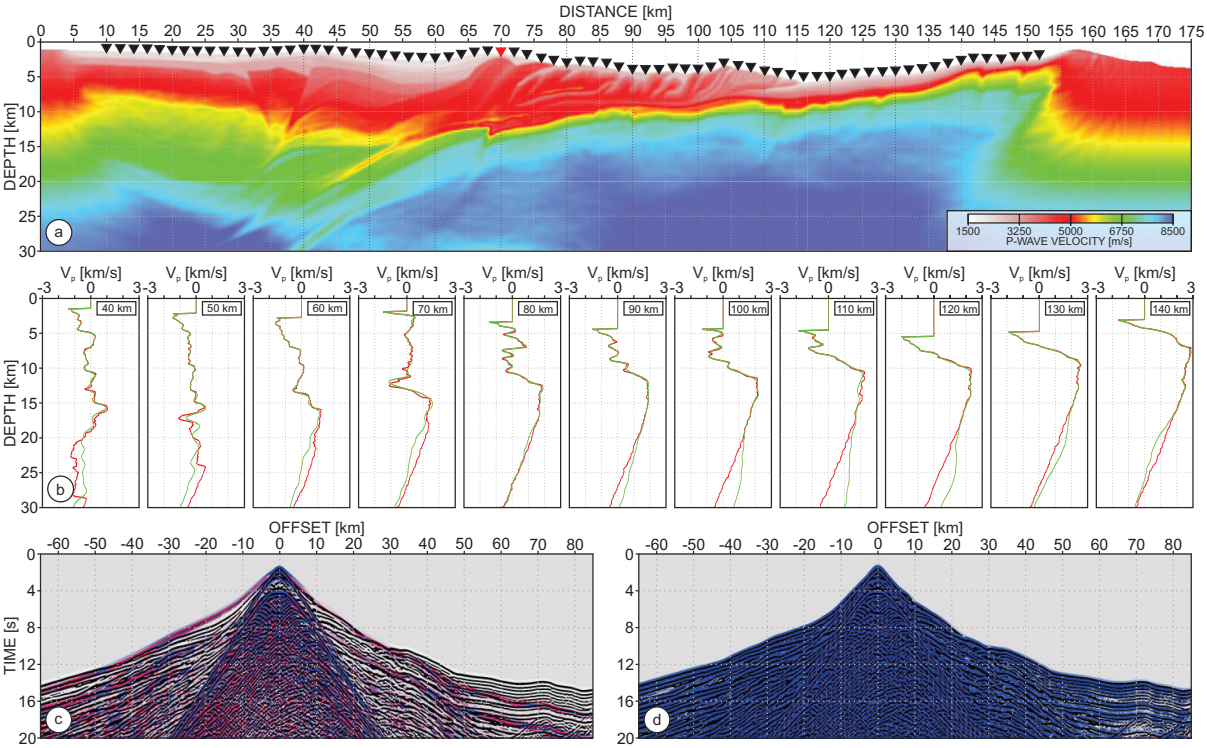

Figure 3 *(a) Final V_p model after STAGE 4; (b) True (red) and reconstructed (green) V_p perturbation logs; (c)-(d) Comparison of the data-fitting at the initial and the final stage. Observed data (black phases) are superimposed over synthetic data (plotted in red-blue).*

Acknowledgements

This study was partially funded: (i) by the SEISCOPE consortium (*http://seiscope2.osug.fr*), sponsored by AKERBP, CGG, CHEVRON, EQUINOR, EXXON-MOBIL, JGI, PETROBRAS, SCHLUMBERGER, SHELL, SINOPEC, SISPROBE, and TOTAL; (ii) the Polish National Science Center, (grant no: 2019/33/ B/ST10/01014). The study was granted access to the HPC PL-Grid Infrastructure (grant id: 3dwind).

References

Aghamiry, H., Gholami, A. and Operto, S. [2018] Improving full-waveform inversion by wavefield reconstruction with alternating direction method of multipliers. *Geophysics*, **84**.

Bertsekas, D.P. and Castanon, D. [1989] The auction algorithm for the transportation problem. *Annals of Operations Research*, **20**(1), 67–96.

Górszczyk, A. and Operto, S. [2020] GO_3D_OBS - The Nankai Trough-inspired crustal-scale benchmark for the next generation 3D seismic surveys design and the imaging methods validation. *Geoscientific Model Development*, (to be submitted).

Górszczyk, A., Operto, S. and Malinowski, M. [2017] Toward a robust workflow for deep crustal imaging by FWI of OBS data: The eastern Nankai Trough revisited. *Journal of Geophysical Research: Solid Earth*, **122**(6), 4601–4630.

Métivier, L., Brossier, R., Mérigot, Q. and Oudet, E. [2019] A graph space optimal transport distance as a generalization of L^p distances: application to a seismic imaging inverse problem. *Inverse Problems*, **35**(8), 085001.

Sambolian, S., Operto, S., Ribodetti, A., Tavakoli F., B. and Virieux, J. [2018] Parsimonious slope tomography based on eikonal solvers and the adjoint-state method. In: *Expanded Abstracts, 80th Annual EAGE Meeting (Copenhagen)*.